

33 **Abstract:**

34 Humans have bred different lineages of domestic dogs for different tasks, like hunting, herding,
35 guarding, or companionship. These behavioral differences must be the result of underlying neural
36 differences, but surprisingly, this topic has gone largely unexplored. The current study examined
37 whether and how selective breeding by humans has altered the gross organization of the brain in dogs.
38 We assessed regional volumetric variation in MRI studies of 62 male and female dogs of 33 breeds.
39 Notably, neuroanatomical variation is plainly visible across breeds. This variation is distributed non-
40 randomly across the brain. A whole-brain, data-driven independent components analysis established
41 that specific regional sub-networks covary significantly with each other. Variation in these networks is
42 not simply the result of variation in total brain size, total body size, or skull shape. Furthermore, the
43 anatomy of these networks correlates significantly with different behavioral specialization(s) such as
44 sight hunting, scent hunting, guarding, and companionship. Importantly, a phylogenetic analysis
45 revealed that most change has occurred in the terminal branches of the dog phylogenetic tree,
46 indicating strong, recent selection in individual breeds. Together, these results establish that brain
47 anatomy varies significantly in dogs, likely due to human-applied selection for behavior.

48

49 **Significance statement:**

50 Dog breeds are known to vary in cognition, temperament, and behavior, but the neural origins of this
51 variation are unknown. In an MRI-based analysis, we found that brain anatomy covaries significantly
52 with behavioral specializations like sight hunting, scent hunting, guarding, and companionship.
53 Neuroanatomical variation is not simply driven by brain size, body size, or skull shape, and is focused in
54 specific networks of regions. Nearly all of the identified variation occurs in the terminal branches of the
55 dog phylogenetic tree, indicating strong, recent selection in individual breeds. These results indicate
56 that through selective breeding, humans have significantly altered the brains of different lineages of
57 domestic dogs in different ways.

58

59

60 Introduction

61 A major goal of modern neuroscience is to understand how variation in behavior, cognition, and
62 emotion relates to underlying neural mechanisms. A massive “natural experiment” in this arena has
63 been right under our noses: domestic dogs. Humans have selectively bred dogs for different, specialized
64 abilities – herding or protecting livestock; hunting by sight or smell; guarding property or providing
65 companionship. Significant breed differences in temperament, trainability, and social behavior are
66 readily appreciable by the casual observer, and have also been documented quantitatively (e.g., (Serpell
67 and Hsu 2005, Tonoike, Nagasawa et al. 2015)). Furthermore, recent genetic research indicates that this
68 behavioral variation is highly heritable (MacLean, Snyder-Mackler et al. 2019).

69 This panoply of behavioral specializations *must* rely on underlying neural specializations. A small
70 number of studies have investigated neural variation in dogs, including, for example, the effects of skull
71 shape on brain morphology (e.g., (Carreira and Ferreira 2015, Pilegaard, Berendt et al. 2017) and
72 anatomical correlates of aggression (e.g., (Jacobs, Van Den Broeck et al. 2007, Vage, Bonsdorff et al.
73 2010)). However, the neural underpinnings of behavioral differences between breeds remain largely
74 unknown.

75 Most modern dog breeds were developed in an intentional, goal-driven manner relatively recently in
76 evolutionary time; estimates for the origins of the various modern breeds vary between the past few
77 thousand to the past few hundred years (Larson, Karlsson et al. 2012). This strong selection pressure
78 suggests that brain differences between breeds may be closely tied to behavior. However, selection
79 also occurred for outward physical appearance, including craniofacial morphology. This may have
80 placed constraints on the internal dimensions of the skull, which in turn may have had secondary effects
81 on brain morphology. There is substantial diversification of skull shape across dog breeds, and this has
82 been linked to behavioral differences (Drake and Klingenberg 2010, McGreevy, Georgevsky et al. 2013).
83 Alternatively, neuroanatomical variation may be explained primarily by body size rather than breed
84 membership, with different breeds’ brains representing minor, random, scaled-up or scaled-down
85 variants of a basic species-wide pattern.

86 Any attempt to determine whether breeding for behavior has altered dog brains would have to be able
87 to differentiate between these competing (and potentially interacting) hypotheses. A simple
88 comparison of regional volumes would be insufficient for several reasons. First, a significant difference
89 in the volume of, for example, the amygdala in pit bulls versus golden retrievers might seem intuitively
90 meaningful, but in order to ascertain whether such a difference was truly the result of selection pressure
91 on behavior, the phylogenetic structure of the dog family tree needs to be taken in to account in order
92 to partition variance attributable to inheritance, and equal statistical priority needs to be given to the
93 alternative hypotheses that observed variation in morphology. Second, and perhaps most importantly,
94 a priori comparisons of regional gray matter volumes presuppose that experimenters can identify
95 meaningful borders between regions. For highly conserved structures with clear anatomical boundaries,
96 like the amygdala, this task is surmountable – but very little is known about the organization of higher-
97 order cortical regions in dogs, and some complex behaviors that are the focus of selective breeding, like

98 herding or interspecies communication, almost certainly rely on some of these areas. For this reason,
 99 even creating the regional outlines for a simple ROI analysis would be problematic.

100 Therefore, the current study took a totally data-driven, whole-brain, agnostic approach to assessing
 101 morphological variation across dog brains. Our goal was to (a) determine whether significant non-
 102 random variation in brain anatomy exists across dogs, and if so, (b) differentiate between the competing
 103 and possibly interacting explanations for this variation.

104

105 **Materials and Methods**

106

107 Subjects

108 The dataset included T2-weighted MRI scans from 62 purebred dogs of 33 different breeds. These were
 109 grouped into 10 different breed groups as defined by American Kennel Club, which ostensibly represent
 110 groupings that were developed for similar behavioral specializations, such as herding or hunting. **Table**
 111 **1** lists the breed, breed group, and other data for all dogs included in the study.

112

ID	Breed	Sex	Age (years)	Body mass (kg)	Cephalic index (from database)	Neuro- cephalic index	Brain volume (mm ³)	Ostensible behavioral specialization / purpose
1	Basset Hound	Male	4.0	28.1	0.74	51.89	100070.10	scent hunting
2	Beagle	Male	14.3	17.0	0.74	61.82	82750.29	scent hunting
3	Beagle	Male	4.0	11.7	0.76	61.82	64887.65	scent hunting
4	Beagle	Male	ND	28.5	0.85	61.82	23259.63	scent hunting
5	Beagle	Male	4.0	8.3	0.82	61.82	66733.96	scent hunting
6	Beagle	Male	1.7	28.5	0.78	61.82	65738.93	scent hunting
7	Bichon Frise	Male	9.0	9.3	0.80	61.51	61849.71	explicit companionship
8	Border Collie	Male	6.1	28.2	0.65	54.38	83215.10	herding
9	Border Collie	Male	5.6	20.6	0.65	54.38	81668.60	herding
10	Boston Terrier	Male	11.9	12.5	0.90	92.62	66301.82	explicit companionship vermin control sport fighting
11	Boston Terrier	Male	5.8	8.9	0.90	92.62	76426.61	explicit companionship vermin control sport fighting
12	Boxer	Male	8.1	31.8	0.68	67.19	81555.33	guarding/protecting/sentinel work police/military work, war

									sport fighting
13	Boxer	Male	5.0	34.2	0.67	67.19	80814.97		guarding/protecting/sentinel work police/military work, war sport fighting
14	Boxer	Female	10.7	31.8	0.83	66.28	93337.26		guarding/protecting/sentinel work police/military work, war sport fighting
15	Boxer	Male	9.3	40.8	0.70	67.19	82323.66		guarding/protecting/sentinel work police/military work, war sport fighting
16	Bulldog	Male	1.0	16.8	0.74	90.18	63154.13		explicit companionship sport fighting
17	Bulldog	Male	4.4	30.0	0.77	90.18	80128.00		explicit companionship sport fighting
18	Cavalier King Charles Spaniel	Female	0.5	3.2	0.81	76.77	55777.97		explicit companionship
19	Cavalier King Charles Spaniel	Female	0.5	14.5	0.92	76.77	64695.16		explicit companionship
20	Cocker Spaniel	Female	6.4	18.1	0.75	61.01	66708.41		bird retrieval
21	Dachsund	Female	11.3	4.9	0.79	51.76	44076.29		vermin control scent hunting
22	Dachsund	Female	6.6	6.4	0.77	51.76	60492.56		vermin control scent hunting
23	Dachsund	Male	7.8	5.6	0.81	49.59	57168.79		vermin control scent hunting
24	Dachsund	Female	1.8	5.3	0.81	51.76	49716.87		vermin control scent hunting
25	Doberman Pinscher	Female	4.7	29.8	0.62	46.96	80287.44		guarding/protecting/sentinel work police/military work, war
26	English Pointer	Male	7.3	27.3	0.74	ND	91448.24		bird retrieval
27	German Short Haired Pointer	Female	6.2	27.0	0.73	48.30	75612.46		bird retrieval
28	Golden Retriever	Male	10.0	39.8	0.69	56.52	96010.49		bird retrieval
29	Golden Retriever	Male	6.0	42.2	0.70	56.52	96941.92		bird retrieval
30	Golden Retriever	Male	11.0	34.9	0.68	56.52	86438.69		bird retrieval
31	Greyhound	Female	7.5	36.7	0.65	45.83	97610.47		sight hunting
32	Greyhound	Male	3.8	37.1	0.65	46.84	97774.89		sight hunting
33	Greyhound	Female	2.2	36.0	0.66	45.83	101969.38		sight hunting

34	Jack Russell Terrier	Male	ND	14.0	0.80	59.28	70125.35	vermin control
35	Keeshound	Male	7.2	21.6	0.71	60.18	68766.94	explicit companionship guarding/protecting/sentinel work
36	Labrador Retriever	Male	9.7	32.6	0.65	55.82	94762.33	bird retrieval
37	Labrador Retriever	Female	5.0	30.5	0.66	56.11	84161.70	bird retrieval
38	Lhasa Apso	Female	10.7	13.2	0.93	ND	58177.18	guarding/protecting/sentinel work
39	Lhasa Apso	Female	4.0	7.6	0.86	ND	58152.92	guarding/protecting/sentinel work
40	Maltese	Male	6.6	6.0	0.81	65.29	46642.03	explicit companionship
41	Maltese	Male	10.0	3.0	0.84	65.29	35280.20	explicit companionship
42	Maltese	Male	5.5	6.6	0.77	65.29	46629.97	explicit companionship
43	Maltese	Male	6.0	8.9	0.88	65.29	47610.27	explicit companionship
44	Maltese	Female	6.0	2.0	0.92	68.83	28052.45	explicit companionship
45	Maltese	Female	4.9	3.4	0.85	68.83	46330.73	explicit companionship
46	Miniature Schnauzer	Male	9.4	12.8	0.77	51.79	62053.63	vermin control
47	Miniature Schnauzer	Female	6.3	5.0	0.80	54.99	53517.22	vermin control
48	Old English Sheepdog	Male	3.7	33.1	0.69	54.39	80709.26	herding
49	Pit Bull	Male	2.1	27.1	0.72	69.96	80571.31	sport fighting
50	Siberian Husky	Female	3.0	18.1	0.67	55.17	62094.04	running/racing
51	Silky Terrier	Male	3.0	4.4	0.84	58.23	46832.08	vermin control
52	Springer Spaniel	Female	1.1	18.4	0.75	49.34	72442.26	bird retrieval
53	Standard Poodle	Female	7.9	22.6	0.73	ND	80235.75	bird retrieval
54	Weimaraner	Male	3.3	48.4	0.66	49.05	110812.36	sight hunting
55	Welsh Corgi	Male	5.6	15.1	0.72	63.09	83234.19	herding
56	West Highland White Terrier	Male	5.9	11.0	0.78	60.84	72254.08	vermin control
57	Wheaton Terrier	Male	7.0	19.2	0.71	ND	70234.47	guarding/protecting/sentinel work herding vermin control bird retrieval
58	Whippet	Female	15.5	13.6	0.72	50.60	71357.64	sight hunting
59	Yorkshire Terrier	Female	3.8	3.9	0.82	ND	45103.02	explicit companionship vermin control
60	Yorkshire	Male	13.0	4.2	0.81	ND	45217.54	explicit companionship

	Terrier							vermin control
61	Yorkshire Terrier	Male	0.8	3.5	0.79	ND	38163.05	explicit companionship vermin control
62	Yorkshire Terrier	Male	11.5	3.2	0.82	ND	51760.84	explicit companionship vermin control

113

114 **Table 1.** Data for all dogs used in the study. Dogs from mixed/unknown breeds were excluded from analyses that used breed
 115 group as an independent variable. Cephalic indices are sex- and breed-specific averages from a large public database (Stone,
 116 McGreevy et al. 2016). Missing data denoted with “ND”.

117

118 Image acquisition and preprocessing

119

120 T2-weighted MRI images were acquired on a 3.0T GE HDx MRI unit with a GE 5147137-2 3.0T HD T/R
 121 Quad Extremity Coil. Images were opportunistically collected at the Veterinary Teaching Hospital at the
 122 University of Georgia at Athens from dogs that were referred for neurological examination but were not
 123 found to have any neuroanatomical abnormalities. All scans were re-reviewed by a board-certified
 124 veterinary neurologist before inclusion.

125

126 The preprocessing pipeline was implemented using the NiPype workflow engine (Gorgolewski, Burns et
 127 al. 2011). Both transverse-acquired and sagittally-acquired images were available for each dog.
 128 Transverse-acquired images ranged from 0.234 mm² in-plane resolution and 2.699 mm slice distance to
 129 0.352 mm² in-plane resolution and 3.499 mm slice distance. Sagittally-acquired images ranged from
 130 0.273 mm² in-plane resolution and 3.200 mm slice distance to 0.430 mm² in-plane resolution and 3.200
 131 mm slice distance. To maximize the use of all available anatomical information, the transverse and
 132 sagittal images were combined as follows. First, we manually performed skull-stripping on the
 133 transverse image. Next, we determined the smallest region of interest (ROI) that completely covered
 134 the brain from the brain mask image. The transverse image and transverse brain mask were then
 135 cropped using the computed ROI coordinates. Then, the transverse images were resampled to produce
 136 isotropic voxels in all three dimensions, the sagittal image was resliced so that it was in the same
 137 orientation as the transverse images, and a rigid registration was computed from the sagittally-acquired
 138 image to the original transverse image. The region containing the brain was then cropped in the sagittal
 139 image, and we then registered the smaller cropped sagittal image to the isotropically-resampled
 140 transverse brain image using a rigid registration. Finally, the cropped transverse and sagittal images
 141 were then rescaled so that the robust mean intensity of both images was 100, the images were
 142 averaged together, and then the brain mask applied to this combined image. A general diagram
 143 illustrating the overall processing pipeline is included in **Figure 1-1**, and a detailed NiPype registration
 144 workflow is included in **Figure 1-2**, both available in the extended data. Additionally, the accompanying
 145 registration code is available at <https://gist.github.com/dgutman/a0e05028fab9c6509a997f703a1c7413>.

146

147 Template creation

148

149 We produced a study-specific template representing the average brain morphology across the entire
150 group, equally unbiased toward any particular image. This was accomplished using the
151 *buildtemplateparallel.sh* script in the ANTS software package (Avants, Tustison et al. 2009), which
152 nonlinearly registers each image into a common spatial framework.

153

154 Experimental design and statistical analyses

155

156 *Morphological analyses*

157

158 During nonlinear registration, a warpfield is produced that represents the mapping from the original
159 image to the target image. The Jacobian of the warpfield represents the degree of warping that had to
160 occur in each original image in order to bring it into alignment with the target image. To localize
161 significant variation in gray matter morphology, we applied a one-sample t-test on the demeaned log
162 Jacobian determinant images. This was accomplished using FSL's *randomise*, a tool for Monte Carlo
163 permutation testing on general linear models (Winkler, Ridgway et al. 2014). This analysis permutes the
164 sign of the log Jacobian and tests the null hypothesis that variation from the mean is random and
165 therefore symmetrically distributed and centered around zero. The resultant t-statistic image was
166 thresholded at $p < 0.05$, after multiple comparisons correction was carried out using threshold-free
167 cluster enhancement (Smith and Nichols 2009).

168

169 To calculate neurocephalic index, we identified maximally distant points on the left-right, rostral-caudal,
170 and dorsal-ventral axes; neurocephalic index was computed the ratio of brain width to brain length x
171 100.

172

173 Cephalic index is defined as the ratio of skull width to skull length x 100. For many scans in our
174 database, the exterior of the skull was not visible, but a large database of skull measurements is publicly
175 available (Stone, McGreevy et al. 2016). We computed male and female average cephalic indices
176 separately for each breed and used these sex-specific, breed-average measures in our analyses.

177

178 To identify regional co-variation in gray matter morphology, we used GIFT, a software package for
179 Matlab (Calhoun, Adali et al. 2001). GIFT's toolbox for source-based morphometry (SBM) (Xu, Groth et
180 al. 2009) is a multivariate alternative to voxel-based morphometry (VBM). It uses independent
181 components analysis to identify spatially distinct, distributed networks of regions that covary across
182 individuals, and computes their statistical relationship to other categorical or continuous variables. T2-
183 weighted images underwent bias field correction using ANTS's Atropos N4 tool (Avants, Tustison et al.
184 2011) and segmentation into gray matter, white matter, and cerebrospinal fluid using FSL's FAST tool
185 (Zhang, Brady et al. 2001). Gray matter segmentations were warped to the study-specific template and
186 modulated by their log Jacobian determinants to produce per-subject maps of the degree of
187 morphological divergence from the study-specific group-average template. In other words, the input to
188 SBM consisted of gray matter maps for each subject, where intensity at each voxel corresponded to the
189 degree of deformation required in order to come into alignment with the template (i.e., the demeaned
190 log Jacobians). The number of sources was estimated using Akaike's information criterion (AIC, (Akaike

191 1974)); the application of AIC in SBM is described in (Xu, Groth et al. 2009). This procedure identified six
192 components, each of which were thresholded at Z scores above 1.96 or below -1.96. Multiple
193 regression and ANOVA analyses were then used to compute the relationship of each component to
194 American Kennel Club-defined breed groups, with the statistical threshold set at $p < 0.05$ after multiple
195 comparisons correction.

196

197 *Phylogenetic statistics*

198

199 Because comparative data may be non-independent due to shared phylogenetic history, the
200 assumptions of standard statistical methods may be violated (Harvey and Pagel 1991). We therefore
201 used phylogenetic comparative methods that account for phylogenetic non-independence by including
202 expected phylogenetic variance-covariance among species into the error term of generalized least-
203 squares ('pGLS') linear models (Rohlf 2001). When quantifying linear models we additionally included a
204 lambda parameter to account for phylogenetic signal (Pagel 1997). To test for differences in statistical fit
205 among linear models that include different parameters (for example, the inclusion of grouping variables
206 to test for differences among breed groups), we used least-squares phylogenetic analysis of covariance
207 (pANCOVA) (Smaers and Rohlf 2016, Smaers and Mongle 2018). It should be noted that 'phylogenetic'
208 approaches such as pGLS and pANCOVA are interpreted in the same way as standard least-squares
209 approaches. The only difference between standard and phylogenetic least-squares approaches is that
210 the phylogenetic approaches weight data points according to phylogenetic relatedness (Rohlf, 2001).

211 We further investigated the relationship between morphological components and the phylogenetic tree
212 by estimating the amount of change that occurs on each lineage using a multiple variance Brownian
213 motion approach (Smaers, Mongle et al. 2016, Smaers and Mongle 2018). This approach estimates
214 phenotypic change along individual lineages of a tree and has been shown to provide more accurate
215 estimates than traditional ancestral estimation methods (Smaers and Mongle 2017).

216 Lastly, we use multi-regime Ornstein-Uhlenbeck ('OU') approaches to estimate phylogenetic shifts in
217 mean value directly from the data. This approach has become a standard approach in comparative
218 biology to model trait change across a phylogeny. Specifically, this approach quantifies the evolution of
219 a continuous trait 'X' as $dX(t) = \alpha[\theta - X(t)]dt + \sigma dB(t)$ where ' σ ' captures the stochastic evolution of
220 Brownian motion, ' α ' determines the rate of adaptive evolution towards an optimum trait value ' θ ' (90).
221 This standard OU model has been modified into multiple-regime OU models allowing optima to vary
222 across the phylogeny (Butler and King 2004). Such multi-regime OU models allow modelling trait
223 evolution towards different 'regimes' that each display a different mean trait value. In other words,
224 these approaches allow estimating directly from the data where in a phylogeny a shift in mean value of
225 a trait has occurred. To overcome inherent difficulties with optimizing OU parameters (Ho and Ane
226 2014), several algorithmic improvements have been proposed. Here, we use the approach proposed by
227 Khazzazian et al. (2016).

228 **Results**

229 Neuromorphological variation is plainly visible across breeds. Midline sagittal images from the raw,
230 native-space scans of selected dogs are shown in **Figure 1A**. To provide a common spatial reference for
231 measuring this variation, we created an unbiased, diffeomorphic template using the ANTS software
232 package (Avants, Tustison et al. 2009). This template represents the average brain for the entire
233 dataset, and is shown in **Figure 1B**.

234 To visualize morphological variation in a more standardized manner, we nonlinearly warped the
235 template to each dog's native-space image. This allowed us to examine breed variation in brain
236 morphology and size with invariant contrast and resolution. We also additionally re-scaled these images
237 to have constant rostral-caudal lengths. This allowed us to more clearly visualize variation in
238 morphology independent from variation in size. Both sets of scaled template images are shown in
239 **Figure 1A**.

240 To carry out quantitative assessments of regional variation in gray matter morphology, we used the
241 Jacobian determinants of the native-space-to-template spatial deformation fields to produce a variation
242 intensity map. These fields represent a map of where and how much each dog's scan had to adjust in
243 order to become aligned to the group-average template. The standard deviation of these maps thus
244 indexes the extent to which brain anatomy varies across individuals, and is shown in **Figure 1C**.

245 To determine whether this variation was randomly distributed across the brain or focused in specific
246 areas, we applied Monte Carlo permutation testing on the demeaned Jacobian determinant images.
247 Importantly, this revealed that a large proportion of the brain shows significant gray matter
248 morphological variation across subjects, illustrated in **Figure 1D**.

249

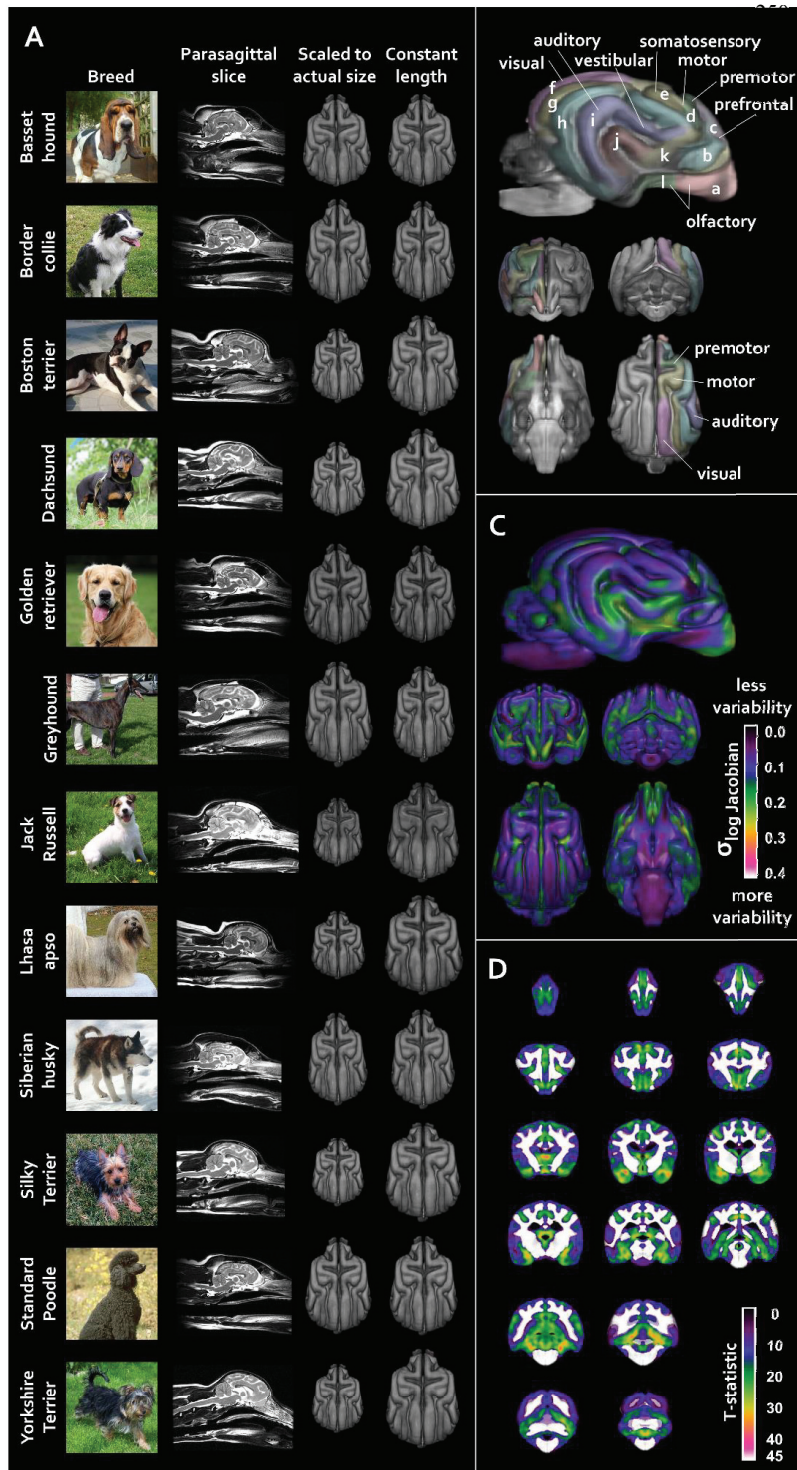


Fig. 1. Neuroanatomical variation in domestic dogs.

(A) MRI images and 3D reconstructions of warped template from 10 selected dogs of different breeds. Public-domain photos from Wikimedia Commons.

(B) Unbiased group-average template for this dataset. See Figures 1-1 and 1-2 for processing schematics.

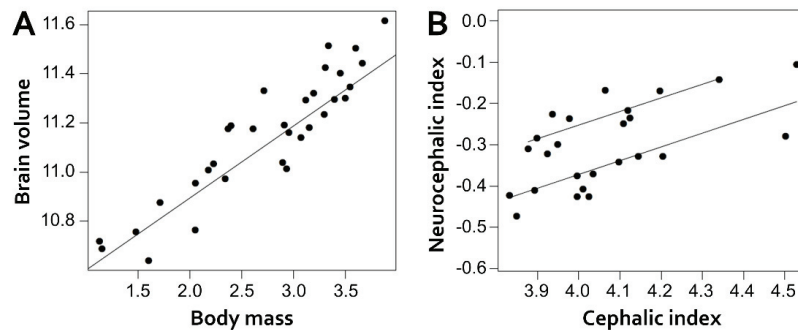
Neuroanatomical labels (based on (Palazzi 2011, Datta, Lee et al. 2012, Evans and de Lahunta 2013)): a) olfactory peduncle; b) orbital (presylvian) gyrus; c) proreal gyrus; d) pre cruciate gyrus; e) postcruciate gyrus; f) marginal (lateral) gyrus; g) ectomarginal gyrus; h) suprasylvian gyrus; i) ectosylvian gyrus; j) sylvian gyrus; k) insular cortex; l) piriform lobe.

(C) Brain-wide morphological variation, regardless of breed, as indexed by the standard deviation of all dogs' Jacobian determinant images.

(D) A Monte Carlo permutation test on demeaned gray matter Jacobian determinant images revealed that much of gray matter shows significant deviation from group-mean morphology. Colored regions are all $p < .05$ after multiple comparison correction; T statistic values are illustrated.

301 Given these results, we next sought to determine what accounts for this variation by probing the extent
 302 to which it is related to body size, head shape, and/or breed group membership.

303 **Figure 2A** shows the relationship between brain volume and body mass. The scaling coefficient of this
 304 relationship (pGLS; $b=0.231$, 95% CI=0.26-0.36) is significantly lower than that observed across most
 305 mammals (~ 0.67), indicating the occurrence of more variation in body size relative to variation in brain
 306 size than would be expected. Importantly, using the tree structure from a recent large-scale genomic
 307 analysis (Parker, Dreger et al. 2017), we were able to determine that the phylogenetic signal of the
 308 brain-body allometry is negative – i.e., that variation present at the tree’s terminal branches is not
 309 predicted by the deeper structure of the tree. If grade shifts in the brain-body allometry exist, these
 310 would putatively show differences among different breeds. We tested this hypothesis by estimating
 311 putative grade shifts in the brain to body allometry directly from the data using an OU modelling
 312 approach (Khabbazian, Kriebel et al. 2016). This analysis revealed no grade shifts, thereby indicating that
 313 a one-grade allometry is the best explanation of the bivariate brain to body relationship.



314

315 **Fig. 2. Phylogenetic generalized least squares (pGLS) analyses on gross brain, body, and skull measurements.** (A) Brain
 316 volume vs. body mass. (B) Neurocephalic index vs. cephalic index. Plotted points represent breed averages, not individuals.

317 In mammals, head shape is commonly measured using cephalic index (also known as skull index),
 318 calculated as maximum head width divided by maximum head length. We were interested in the
 319 possibility that human-driven selection on external craniofacial morphology may have had on the
 320 internal dimensions of the skull. To assess this, we computed an analogous *neurocephalic* index for each
 321 dog (maximum internal cranial cavity length divided by maximum internal cranial cavity width). **Figure**
 322 **2B** shows the relationship between neurocephalic and cephalic index. Cephalic index is a significant
 323 predictor of neurocephalic index (pGLS: $b=0.37$, $t=3.70$, $p<0.01$). Also here we questioned whether grade
 324 shifts in this allometry exist, putatively showing differences among breeds. This analysis revealed that
 325 the neurocephalic-cephalic allometry was thus best explained by a two-grade model ($F=31.19$, $p<0.001$).
 326 The breeds on the higher grade, with a greater neurocephalic index for a given cephalic index, were as
 327 follows: Basset hound, beagle, German short-haired pointer, dachshund, cavalier King Charles spaniel,
 328 springer spaniel, west highland white terrier, silky terrier, bichon frise, and maltese. Importantly, this
 329 grade difference in the neurocephalic to cephalic index aligns with a significant difference in body size

330 (pANOVA: $F=9.73$, $p<0.01$; average body size 11kg, versus 23kg in other breeds). Smaller-bodied dogs
331 hereby have a higher neurocephalic index (more spherical brains) for a given cephalic index (external
332 head shape).

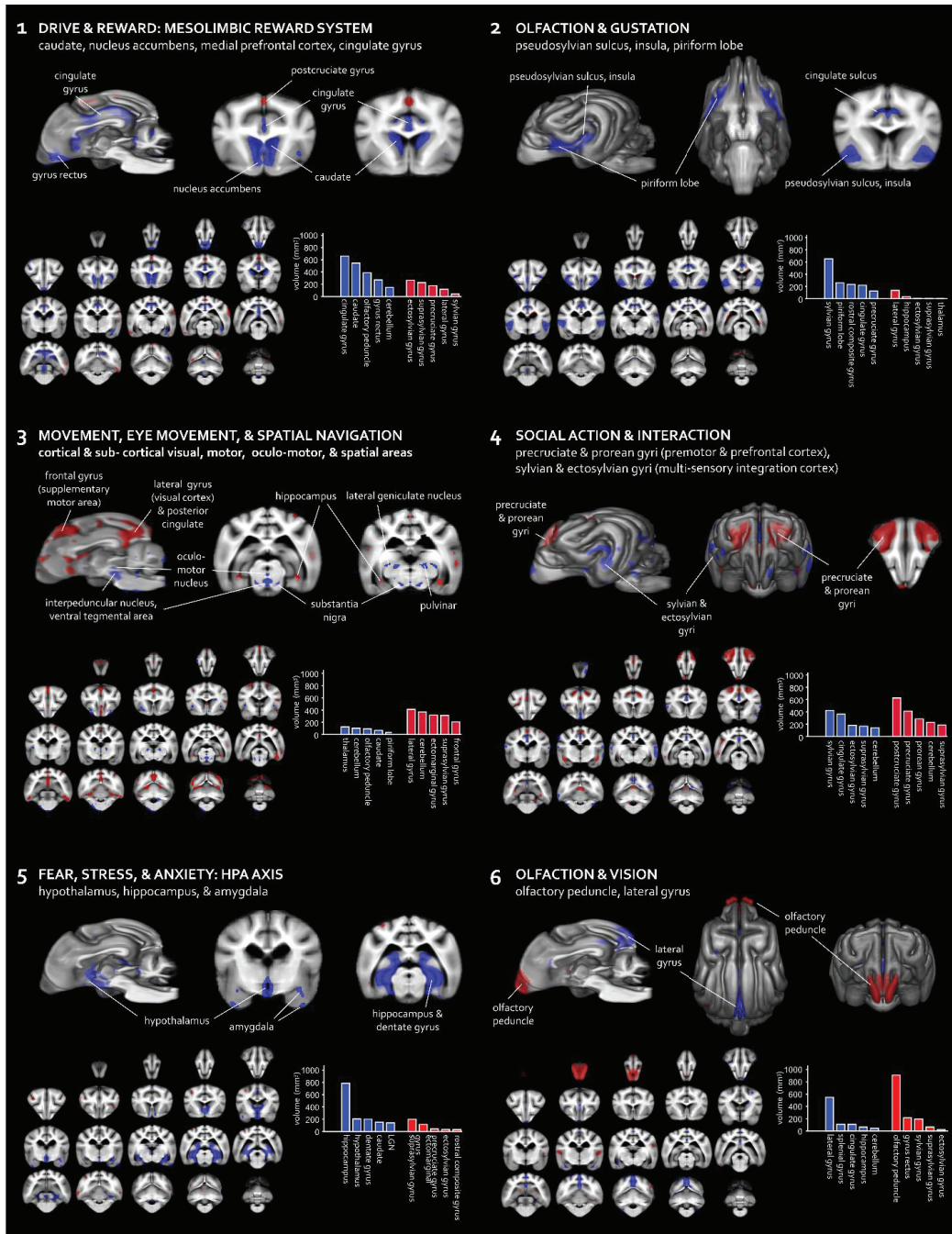
333 If variation in dog brain anatomy is unrelated to behavior, then variation should be randomly distributed
334 across regions. Alternatively, if this variation represents heritable adaptations for behavior, then
335 significant covariance should exist in separable, independent sub-networks of regions. To assess this,
336 we performed source-based morphometry, a multivariate alternative to voxel-based morphometry
337 which makes use of independent components analysis. This was accomplished using the GIFT software
338 package (Xu, Groth et al. 2009). Results revealed 6 networks where regional volume covaried
339 significantly across individuals. **Figure 3** shows these networks, along with factor loadings for each
340 breed group. Major anatomical constituents of each network are labeled. Additional research is needed
341 to definitively link the function of each network to its adaptive role in response to behavior selection.
342 However, we note putative roles which may serve as initial hypotheses for future research.

343 Network 1 includes the nucleus accumbens, dorsal and ventral caudate, cingulate gyrus, olfactory
344 peduncle, and gyrus rectus (medial prefrontal cortex). These regions are part of or connected to the
345 mesolimbic reward system, a network implicated in reward signaling related to reinforcement learning,
346 incentive salience, and motivation broadly across species (Alcaro, Huber et al. 2007, O'Connell and
347 Hofmann 2011); in dogs, the caudate nucleus activates for both food reward and human social reward
348 (Cook, Prichard et al. 2016). Tentatively, this network might be relevant for social bonding to humans,
349 training, and skill learning.

350 Network 2 involves brain regions involved in olfaction and gustation, including the piriform lobe, which
351 contains olfactory cortex, and the insula and pseudosylvian sulcus, where the cortical representation of
352 taste is located (Evans and de Lahunta 2013). This component also involves regions of medial frontal
353 cortex, which is involved in downstream or higher-order processing of chemosensation and shows
354 activation in response to olfactory stimulation in awake but not sedated dogs (Jia, Pustovsky et al. 2014).
355 We propose that this network might support volitional (as opposed to instinctive) responses to olfactory
356 and gustatory stimuli.

357 Network 3 includes a distributed network of subcortical regions that are involved movement, eye
358 movement, vision, and spatial navigation, including the lateral geniculate nucleus, pulvinar,
359 hippocampus, cerebellum, oculomotor nucleus, interpeduncular nucleus, ventral tegmental area, and
360 substantia nigra. It also involves cortical regions, including the medial part of the frontal gyrus
361 (supplementary motor area) and the lateral gyrus (visual cortex). Tentatively, this network may reflect a
362 circuit involved in moving through the physical environment.

363



364

365

366

Fig. 3. Covarying regional networks in dog brain morphology. Independent components analysis revealed 6 regional networks where morphology covaried significantly across individuals. Red and blue regions are volumetrically anticorrelated: in

367 individuals where red is larger, blue tends to be smaller, and vice versa. Graphs represent volumetric quantification of the top 5
368 anatomical constituents of each of the 2 portions of each component.

369 Network 4 involves higher-order cortical regions that may be involved in social action and interaction.
370 The precruciate and prorean gyri house premotor and prefrontal cortex, respectively, while the gyrus
371 rectus is part of medial prefrontal cortex. The expansion of frontal cortex has been linked to increased
372 sociality in extant hyena species (Holekamp, Sakai et al. 2007), and notably, the prorean gyrus has been
373 linked to the emergence of pack structure in canid evolution (Radinsky 1969). The sylvian, ectosylvian,
374 and suprasylvian gyri represent regions of lateral sensory cortex situated between gustatory, auditory,
375 and somatosensory cortex (Evans and de Lahunta 2013), and likely contain higher-order association
376 areas related to sensation and perception. In domestic dog fMRI studies, multisensory activation in
377 these regions has been observed during the presentation of dog and human faces and vocalizations
378 (Cuaya, Hernandez-Perez et al. 2016, Andics, Gacsi et al. 2017, Thompkins, Ramaiahgari et al. 2018).

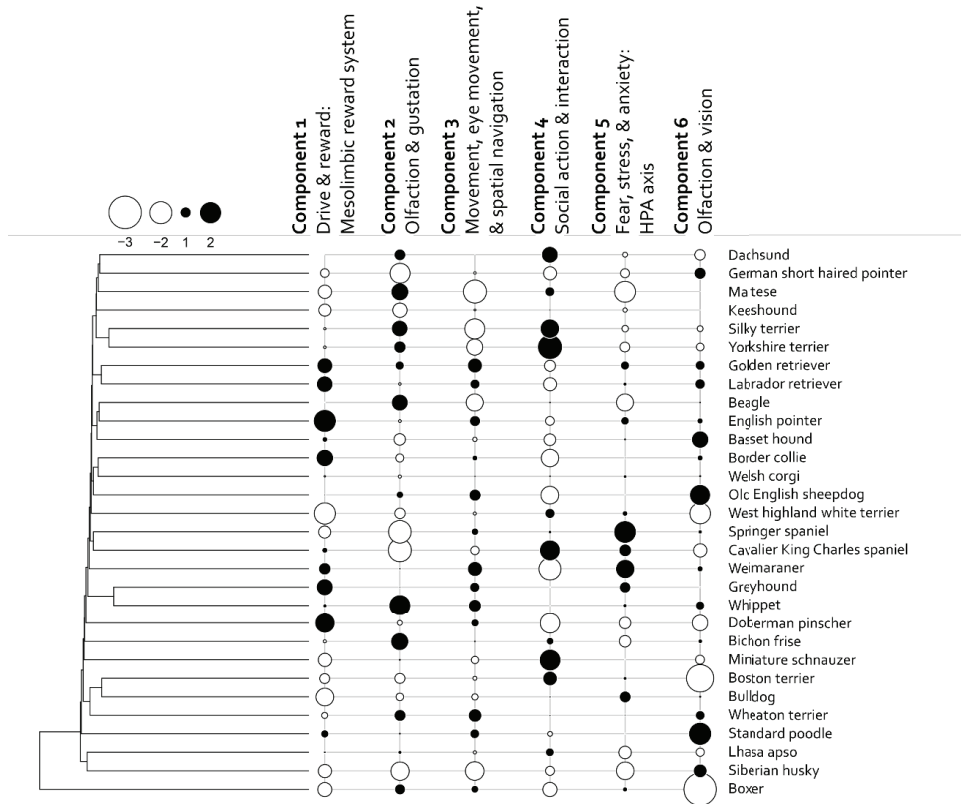
379 Network 5 includes limbic regions that have a well-established role in fear, stress, and anxiety, including
380 the hypothalamus, amygdala, and hippocampus and adjacent dentate gyrus (for a review, see (Tovote,
381 Fadok et al. 2015)). These regions are involved in the HPA axis, which regulates behavioral and
382 endocrine responses to environmental stressors and threats. Some of these regions are also involved in
383 other affective and instinctual processes, including mating, memory, and aggression (O'Connell and
384 Hofmann 2011).

385 Network 6 includes early sensory processing regions for olfaction and vision, including the olfactory
386 peduncle and part of the lateral gyrus, which is the location of primary visual cortex (Evans and de
387 Lahunta 2013).

388 Next, we investigated the relationship between these components, total brain size, and skull
389 morphology. A significant relationship with total brain volume was present for all but Component 6,
390 where it was marginal but did not meet significance (Component 1: $t = 3.663$, $p = 0.001$; Component 2: t
391 $= -2.608$, $p = 0.014$; Component 3: $t = 6.219$, $p < .001$; Component 4: $t = -6.325$, $p < .001$; Component 5: t
392 $= 3.938$, $p < .001$; Component 6: $t = 1.845$, $p = 0.076$). Components 3, 4, and 6 showed significant
393 relationships with cephalic index, while Component 1 was marginal (Component 1: $t = -1.945$, $p = 0.064$;
394 Component 3: $t = -2.165$, $p = 0.041$; Component 4: $t = 2.411$, $p = 0.024$; Component 6: $t = -2.171$, $p =$
395 0.041 ; pGLS). Components 1, 3, 4, and 6 showed significant relationships with neurocephalic index
396 (Component 1: $t = -2.258$, $p = 0.032$; Component 3: $t = -3.823$, $p = 0.001$; Component 4: $t = 7.066$; $p <$
397 $.001$; Component 6: $t = -2.890$, $p = 0.007$, pGLS).

398 We also investigated the relationship between these covarying morphological components and the
399 phylogenetic tree. If variation in brain organization mainly reflects the deep ancestry of the tree, with
400 little relationship to recent behavioral specializations, then brain morphometry should be highly
401 statistically dependent on phylogenetic structure (i.e., high phylogenetic signal). Conversely, if brain
402 organization is strongly tied to selective breeding for behavioral traits, then morphological traits should
403 be divorced from the structure of the tree (i.e., low phylogenetic signal). We observed the latter (**Figure**

404 4). The majority of changes that occur in these components take place on the terminal branches of the
 405 phylogenetic tree.

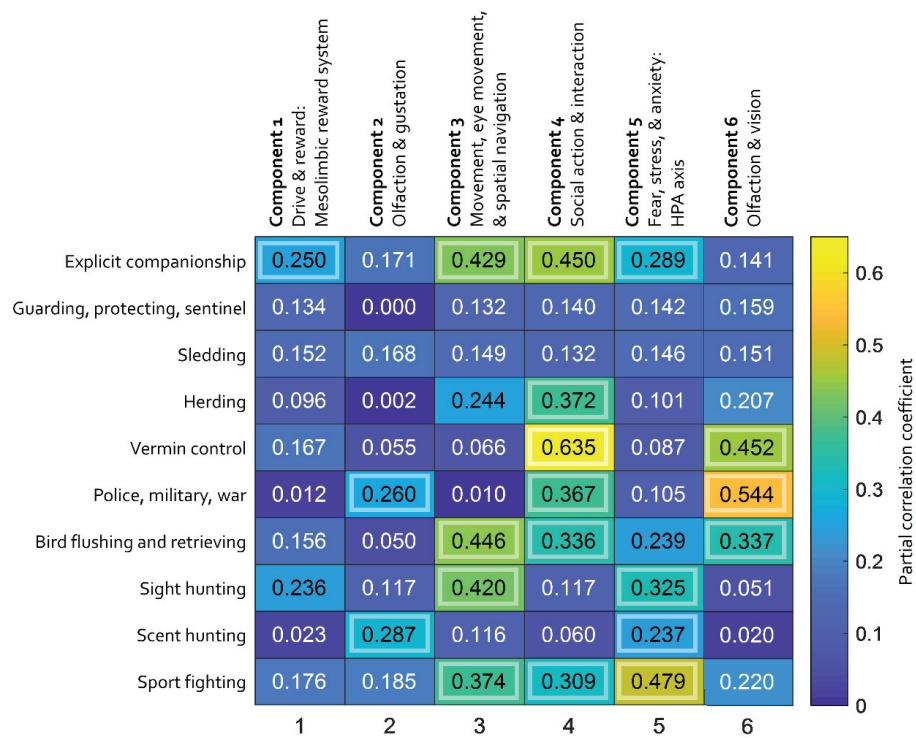


406

407 **Fig. 4. Relationship between morphologically covarying regional brain networks and phylogenetic tree.** Circles indicate
 408 factor loading. Phylogenetic tree from (Parker, Dreger et al. 2017).

409 Finally, we investigated whether these regionally covarying morphological networks were related to
 410 behavior. The American Kennel Club groups individual breeds into breed groups, but these breed
 411 groups change periodically and some groups contain breeds with disparate behavioral functions: for
 412 example, the non-sporting group includes both poodles and shar-peis. Therefore, rather using AKC
 413 breed groups, we identified each individual breed’s ostensible behavioral specialization(s) as noted on
 414 the AKC website (www.akc.org). These were entered into in a multiple regression analysis using the
 415 GIFT Source Based Morphometry toolbox. Each of the 6 components showed significant correlation
 416 with at least one behavioral specialization (**Figure 5**). The behavioral specialization associated with the

417 most components (4 out of 6) was explicit companionship, and the component associated with the most
 418 behavioral specializations (6 out of 10) was Component 4, which involves regions involved in social
 419 action and interaction. Specific associations between associated brain networks and behavioral
 420 specializations are also apparent. For example, Component 3, which involves regions involved in
 421 movement, eye movement, and spatial navigation, showed a significant correlation with sight hunting,
 422 while Network 2, which involves regions involved in olfaction and gustation, showed a significant
 423 correlation with scent hunting.



424

425 **Fig. 5: Relationship between morphologically covarying regional brain networks and ostensible behavioral specializations.**
 426 Colors indicate partial correlation coefficients resulting from multiple regression analysis on source-based morphometry results.
 427 Outlined boxes are significant at $p < .05$.

428

429 **Discussion**

430

431 The current study took a comprehensive, data-driven, agnostic approach to investigating
 432 neuroanatomical variation in domestic dogs. We first questioned whether significant variation in dog
 433 brain morphology even exists. The answer is a clear “yes”: differences in gross brain anatomy are

434 readily appreciable (see **Figure 1A**). This observation was further confirmed by a whole-brain, multiple-
435 comparison-corrected, voxelwise statistical analysis (**Figure 1C-1D**). Having established this basic
436 finding, we then went on to probe the relationship between multiple, potentially interacting factors that
437 might be linked to this variation: the total size of the body or brain, the external and internal
438 morphology of the skull, the structure of the dog phylogenetic tree, and the organization of internal
439 brain networks.

440

441 Dogs show intraspecific variation in morphology to a degree rarely seen in nature. There is a hundred-
442 fold difference between the body mass of a Chihuahua (~1 kg) and the body mass of a Great Dane (~100
443 kg) (Sutter, Mosher et al. 2008). However, we found that dog brain sizes do not scale commensurately
444 to dog body sizes, as indicated by a relatively low scaling coefficient for the relationship between brain
445 size and body mass. To appreciate this effect, consider the adjacent dachshund and golden retriever
446 images in **Figure 1A**: the dachshund's brain takes up most of the available endocranial space, while the
447 golden retriever shows noticeably larger sinuses. A phylogenetic analysis revealed that changes in
448 relative brain size are not predicated by relatedness and are more likely the result of selection on
449 specific terminal branches of the phylogenetic tree (i.e., individual breeds).

450 In comparative animal cognition research, total brain size is often used as a gross index of cognitive
451 capacity. Several previous studies have investigated the relationship between dog body size and
452 cognition or behavior, with apparently contradictory results (see (Helton and Helton 2010, Stone,
453 McGreevy et al. 2016) vs. (Broadway, Samuelson et al. 2017)). Additionally, a study that used a single
454 scaling metric across breeds found that larger-brained (i.e., larger-bodied) dogs performed better on
455 tests of executive function (Horschler, Hare et al. 2019). We found that larger dogs do tend to have
456 larger brains, but that the brain:body allometry across breeds is low, indicating high variability in
457 brain:body ratio across breeds (**Figure 2A**). Furthermore, we found that a substantial amount of
458 variation in internal dog brain morphology is related to total brain size, suggesting that evolutionary
459 increases or decreases in relative brain volume may be driven by changes in specific groups of regions.
460 Moreover, we found that these networks differed across breed groups. Therefore, shifts in relative
461 brain size may be related to expansion or contraction of specific networks, potentially leading to the
462 presence or absence of correlations between body size and behavior depending on the specific breeds
463 or behaviors being studied.

464 We also found that selection for smaller body size has significantly influenced the internal morphology
465 of the cranial cavity. For a given cephalic index, or exterior skull shape, smaller-bodied dogs have more
466 spherical brains (**Figure 2B**). This is consistent with a previous analysis linking foreshortening of the skull
467 to ventral pitching of the brain and olfactory bulb, resulting in a more spherical brain (Roberts,
468 McGreevy et al. 2010). We assessed the extent to which internal and exterior skull morphology were
469 related to the covarying morphometric networks we identified. More networks showed a significant
470 relationship with neurocephalic index than with cephalic index, suggesting that variation in brain
471 morphology appears to be more tied to the internal morphology of the cranial cavity than to external
472 craniofacial morphology – which is perhaps not surprising. Our results indicate that skull morphology is
473 linked to the underlying anatomy of specific, different networks of brain regions; it is possible that this

474 could underlie the reported associations between behavior and head shape (e.g., (Gacsi, McGreevy et al.
475 2009, Helton 2009, McGreevy, Georgevsky et al. 2013)). Not all networks showed a significant
476 relationship with either cephalic index or neurocephalic index, indicating that variation in dog brain
477 morphology is partially but not totally dependent on variation in skull morphology. Importantly, we
478 cannot say from the current analyses whether variation in skull morphology drives variation in brain
479 morphology, the reverse, or both.

480 In addition to these analyses of the gross external shape and size of the brain and skull, we also
481 investigated internal brain organization. This was accomplished using source-based morphometry to
482 identify maximally independent networks that explain the variation present in the dataset. We
483 identified six such networks (**Figure 3**). In the case of circuitry that is highly conserved across species –
484 like circuitry for reward and motivation or fear and anxiety – it is a safe bet that research on other
485 species is a good indicator of the functional role of these systems in dogs. This cannot be assumed to be
486 the case for circuits that involve higher-order cortical association areas. Particularly in the case of our
487 Network 4, it may be tempting to jump to conclusions about parallels with human cortical regions that
488 are located in roughly the same location and are involved in similar tasks, e.g., the fusiform face area,
489 Wernicke’s area, or the mirror system. However, it is important to remember that primates and
490 carnivores diverged further back in time than primates and rodents; humans are more closely related to
491 mice than to dogs. Our last common ancestor with dogs likely had a fairly smooth, simple brain (Kaas
492 2011), and higher-order cortical association areas – along with whatever complex perceptual and
493 cognitive abilities they support – have evolved independently in dogs and humans. Therefore, we stress
494 that the functional roles of these networks, and their relationship to selection on behavior in specific
495 breeds, should at this point still be considered an open question.

496 Having identified these six networks, we then investigated their relationship to the dog phylogenetic
497 tree. We found that the majority of changes that occur in these components take place in the tree’s
498 terminal branches (i.e., individual breeds). This suggests that brain evolution in domestic dog breeds
499 follows an “late burst model,” with directional changes in brain organization being primarily lineage-
500 specific. We also assessed whether these networks were related to selective breeding, as evidenced by
501 the ostensible behavioral specialization(s) of each breed as noted by the AKC. In all six of the regionally
502 covarying networks we found, significant correlations were found with at least one behavioral
503 specialization. Associations between brain networks and related behavioral specializations are
504 apparent. For example, Network 2, which involves regions that support higher-order olfactory
505 processing, shows a significant correlation with scent hunting, while Network 3, which involves regions
506 that support movement, eye movement, and spatial navigation, shows a significant correlation with
507 sight hunting. These findings strongly suggest that humans have altered the brains of different breeds
508 of dogs in different ways through selective breeding.

509 It is important to note that the current study was carried out on opportunistically-acquired data. The
510 dataset included different numbers of dogs from different breeds, and some breeds are not represented
511 at all. We used permutation testing for statistical hypothesis testing, which is a non-parametric
512 approach appropriate for differing group sizes, but it is still possible that different patterns of variation

513 may have been obtained with a different sample makeup. Nonetheless, we expect the basic finding that
514 this variation exists would remain.

515 Additionally, it should be noted that as dogs are increasingly bred to be house pets rather than working
516 animals, selection on behavior is relaxing; significant behavioral differences have been found between
517 working, show, and pet animals within a breed (e.g., (Lofgren, Wiener et al. 2014)). To our knowledge,
518 the dogs in the current study were all house pets. Therefore, the findings reported here should be taken
519 as representative of the innate breed-typical adaptations to brain organization that emerge without the
520 input of specific experience – and may actually reflect relaxed or reduced versions of these adaptations.
521 This might be akin to studying language circuitry in a lineage of language-deprived humans: humans
522 almost certainly have some specialized “hard-wired” adaptations to this circuitry, but experience is
523 required for the anatomical phenotype to fully emerge, and indeed it is difficult to consider language-
524 related neural adaptations divorced from the context of language exposure and learning. Thus, future
525 studies on purpose-bred dogs that are actively performing the tasks for which they are presumably
526 adapted might expect to find additional or more pronounced neuroanatomical effects than we observed
527 here.

528 Together, these findings have relevance to both basic and applied science. First and foremost, our
529 findings introduce neural variation in domestic dog breeds as a novel opportunity for studying the
530 evolution of brain-behavior relationships. Dogs represent a “natural experiment” in behavioral selection
531 which has been ongoing for thousands of years; it seems remarkable that attempts to observe the
532 neurological results of this experiment have so far been fairly minimal. Our findings also have
533 implications for the current proliferation of fMRI studies in pet dogs, which nearly always group
534 together dogs of varying breeds. The current study suggests that this approach might not be ideal,
535 because there may be evolved breed differences in, e.g., functional responses to stimuli or anatomical
536 distribution of receptors. In line with this possibility, one study has already found that border collies and
537 Siberian huskies respond significantly differently to intranasal oxytocin (Kovacs, Kis et al. 2016).
538 Additionally, on a practical level, our findings open the door to brain-based assessment of the utility of
539 different dogs for different tasks. It might be possible, for example, to identify neural features that are
540 linked to different breeds’ specializations for specific behaviors, and to selectively breed or train dogs
541 for enhanced expression of those neural features. Finally, on a philosophical level, these results tell us
542 something fundamental about our own place in the larger animal kingdom: we have been systematically
543 shaping the brains of another species.

544
545
546

547 **References**

548

- 549 Akaike, H. (1974). "A new look at statistical model identification." *IEEE Trans Autom Control* **19**: 716-723.
- 550 Alcaro, A., R. Huber and J. Panksepp (2007). "Behavioral functions of the mesolimbic dopaminergic system: an
551 affective neuroethological perspective." *Brain Res Rev* **56**(2): 283-321.
- 552 Andics, A., M. Gacsi, T. Farago, A. Kis and A. Miklosi (2017). "Voice-Sensitive Regions in the Dog and Human
553 Brain Are Revealed by Comparative fMRI." *Curr Biol* **27**(8): 1248-1249.
- 554 Avants, B., N. Tustison, G. Song and J. Gee (2009). "ANTS: Advanced Open-Source Normalization Tools for
555 Neuroanatomy." *Penn Image Computing and Science Laboratory*.
- 556 Avants, B. B., N. J. Tustison, J. Wu, P. A. Cook and J. C. Gee (2011). "An open source multivariate framework for
557 n-tissue segmentation with evaluation on public data." *Neuroinformatics* **9**(4): 381-400.
- 558 Broadway, M. S., M. M. Samuelson, J. L. Christopher, S. E. Jett and H. Lyn (2017). "Does size really matter?
559 Investigating cognitive differences in spatial memory ability based on size in domestic dogs." *Behav Processes* **138**:
560 7-14.
- 561 Butler, M. A. and A. A. King (2004). "Phylogenetic comparative analysis: A modeling approach for adaptive
562 evolution." *American Naturalist* **164**(6): 683-695.
- 563 Calhoun, V. D., T. Adali, G. D. Pearlson and J. J. Pekar (2001). "A method for making group inferences from
564 functional MRI data using independent component analysis." *Hum Brain Mapp* **14**(3): 140-151.
- 565 Carreira, L. M. and A. Ferreira (2015). "Anatomical Variations in the Pseudosylvian Fissure Morphology of Brachy-
566 , Dolicho-, and Mesaticephalic Dogs." *Anat Rec (Hoboken)* **298**(7): 1255-1260.
- 567 Cook, P. F., A. Prichard, M. Spivak and G. S. Berns (2016). "Awake canine fMRI predicts dogs' preference for
568 praise vs food." *Soc Cogn Affect Neurosci* **11**(12): 1853-1862.
- 569 Cuaya, L. V., R. Hernandez-Perez and L. Concha (2016). "Our Faces in the Dog's Brain: Functional Imaging
570 Reveals Temporal Cortex Activation during Perception of Human Faces." *PLoS One* **11**(3): e0149431.
- 571 Datta, R., J. Lee, J. Duda, B. B. Avants, C. H. Vite, B. Tseng, J. C. Gee, G. D. Aguirre and G. K. Aguirre (2012). "A
572 digital atlas of the dog brain." *PLoS One* **7**(12): e52140.
- 573 Drake, A. G. and C. P. Klingenberg (2010). "Large-scale diversification of skull shape in domestic dogs: disparity
574 and modularity." *Am Nat* **175**(3): 289-301.
- 575 Evans, H. and A. de Lahunta (2013). *Miller's Anatomy of the Dog*, Elsevier Saunders.
- 576 Gacsi, M., P. McGreevy, E. Kara and A. Miklosi (2009). "Effects of selection for cooperation and attention in dogs."
577 *Behav Brain Funct* **5**: 31.
- 578 Gorgolewski, K., C. D. Burns, C. Madison, D. Clark, Y. O. Halchenko, M. L. Waskom and S. S. Ghosh (2011).
579 "Nipype: a flexible, lightweight and extensible neuroimaging data processing framework in python." *Front*
580 *Neuroinform* **5**: 13.
- 581 Harvey, P. H. and M. Pagel (1991). *The comparative method in evolutionary biology*. New York, Oxford University
582 Press.
- 583 Helton, W. S. (2009). "Cephalic index and perceived dog trainability." *Behav Processes* **82**(3): 355-358.
- 584 Helton, W. S. and N. D. Helton (2010). "Physical size matters in the domestic dog's (*Canis lupus familiaris*) ability
585 to use human pointing cues." *Behav Processes* **85**(1): 77-79.
- 586 Ho, L. S. T. and C. Ane (2014). "Intrinsic inference difficulties for trait evolution with Ornstein-Uhlenbeck models."
587 *Methods in Ecology and Evolution* **5**(11): 1133-1146.
- 588 Holekamp, K. E., S. T. Sakai and B. L. Lundrigan (2007). "Social intelligence in the spotted hyena (*Crocuta*
589 *crocuta*)." *Philos Trans R Soc Lond B Biol Sci* **362**(1480): 523-538.
- 590 Horschler, D. J., B. Hare, J. Call, J. Kaminski, A. Miklosi and E. L. MacLean (2019). "Absolute brain size predicts
591 dog breed differences in executive function." *Anim Cogn* **22**(2): 187-198.
- 592 Jacobs, C., W. Van Den Broeck and P. Simoens (2007). "Neurons expressing serotonin-1B receptor in the
593 basolateral nuclear group of the amygdala in normally behaving and aggressive dogs." *Brain Res* **1136**(1): 102-109.
- 594 Jia, H., O. M. Pustovsky, P. Waggoner, R. J. Beyers, J. Schumacher, C. Wildey, J. Barrett, E. Morrison, N. Salibi, T.
595 S. Denney, V. J. Vodyanov and G. Deshpande (2014). "Functional MRI of the olfactory system in conscious dogs."
596 *PLoS One* **9**(1): e86362.
- 597 Kaas, J. H. (2011). "Reconstructing the areal organization of the neocortex of the first mammals." *Brain Behav Evol*
598 **78**(1): 7-21.
- 599 Khabbazian, M., R. Kriebel, K. Rohe and C. Ane (2016). "Fast and accurate detection of evolutionary shifts in
600 Ornstein-Uhlenbeck models." *Methods in Ecology and Evolution* **7**(811-824).

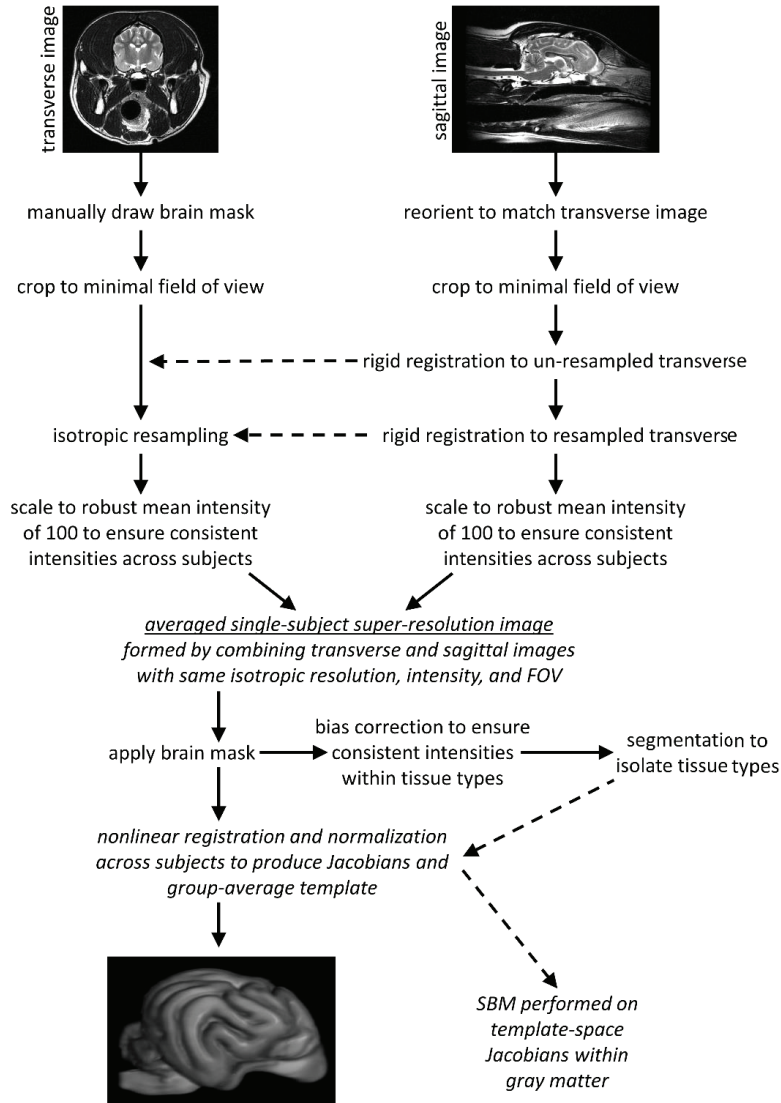
- 601 Kovacs, K., A. Kis, A. Pogany, D. Koller and J. Topal (2016). "Differential effects of oxytocin on social sensitivity
602 in two distinct breeds of dogs (*Canis familiaris*)." *Psychoneuroendocrinology* **74**: 212-220.
- 603 Larson, G., E. K. Karlsson, A. Perri, M. T. Webster, S. Y. Ho, J. Peters, P. W. Stahl, P. J. Piper, F. Lingaas, M.
604 Fredholm, K. E. Comstock, J. F. Modiano, C. Schelling, A. I. Agoulnik, P. A. Leegwater, K. Dobney, J. D. Vigne,
605 C. Vila, L. Andersson and K. Lindblad-Toh (2012). "Rethinking dog domestication by integrating genetics,
606 archeology, and biogeography." *Proc Natl Acad Sci U S A* **109**(23): 8878-8883.
- 607 Lofgren, S. E., P. Wiener, S. Blott, E. Sanchez-Molano, J. A. Wooliams, D. N. Clements and M. Haskell (2014).
608 "Management and personality in Labrador Retriever dogs." *Appl Anim Behav Sci* **156**: 44-53.
- 609 MacLean, E., N. Snyder-Mackler, B. M. VonHoldt and J. A. Serpell (2019). "Highly Heritable and Functionally
610 Relevant Breed Differences in Dog Behavior." *bioRxiv*.
- 611 McGreevy, P. D., D. Georgevsky, J. Carrasco, M. Valenzuela, D. L. Duffy and J. A. Serpell (2013). "Dog behavior
612 co-varies with height, bodyweight and skull shape." *PLoS One* **8**(12): e80529.
- 613 O'Connell, L. A. and H. A. Hofmann (2011). "The vertebrate mesolimbic reward system and social behavior
614 network: a comparative synthesis." *J Comp Neurol* **519**(18): 3599-3639.
- 615 Pagel, M. (1997). "Inferring evolutionary processes from phylogenies." *Zoologica Scripta* **26**: 331-348.
- 616 Palazzi, X. (2011). *The beagle brain in stereotaxic coordinates*, Springer.
- 617 Parker, H. G., D. L. Dreger, M. Rimbault, B. W. Davis, A. B. Mullen, G. Carpintero-Ramirez and E. A. Ostrander
618 (2017). "Genomic Analyses Reveal the Influence of Geographic Origin, Migration, and Hybridization on Modern
619 Dog Breed Development." *Cell Rep* **19**(4): 697-708.
- 620 Pilegaard, A. M., M. Berendt, P. Holst, A. Moller and F. J. McEvoy (2017). "Effect of Skull Type on the Relative
621 Size of Cerebral Cortex and Lateral Ventricles in Dogs." *Front Vet Sci* **4**: 30.
- 622 Radinsky, L. (1969). "Outlines of canid and felid brain evolution." *Ann N Y Acad Sci* **167**: 277-288.
- 623 Roberts, T., P. McGreevy and M. Valenzuela (2010). "Human induced rotation and reorganization of the brain of
624 domestic dogs." *PLoS One* **5**(7): e11946.
- 625 Rohlf, F. J. (2001). "Comparative methods for the analysis of continuous variables: geometric interpretations."
626 *Evolution* **55**(11): 2143-2160.
- 627 Serpell, J. A. and Y. A. Hsu (2005). "Effects of breed, sex, and neuter status on trainability in dogs." *Anthrozoos*
628 **18**(3): 196-207.
- 629 Smaers, J. B. and C. S. Mongle (2017). "On the accuracy and theoretical underpinnings of the multiple variance
630 Brownian motion approach for estimating variable rates and inferring ancestral states." *Biological Journal of the*
631 *Linnean Society* **121**(1): 229-238.
- 632 Smaers, J. B. and C. S. Mongle (2018). "evomap: R package for the evolutionary mapping of continuous traits.
633 Github: <https://github.com/JeroenSmaers/evomap> ".
- 634 Smaers, J. B., C. S. Mongle and A. Kandler (2016). "A multiple variance Brownian motion framework for the
635 estimation of ancestral states and rates of evolution." *Biological Journal of the Linnean Society* **118**: 78-94.
- 636 Smaers, J. B. and F. J. Rohlf (2016). "Testing species' deviation from allometric predictions using the phylogenetic
637 regression." *Evolution* **70**(5): 1145-1149.
- 638 Smith, S. M. and T. E. Nichols (2009). "Threshold-free cluster enhancement: addressing problems of smoothing,
639 threshold dependence and localisation in cluster inference." *Neuroimage* **44**(1): 83-98.
- 640 Stone, H. R., P. D. McGreevy, M. J. Starling and B. Forkman (2016). "Associations between Domestic-Dog
641 Morphology and Behaviour Scores in the Dog Mentality Assessment." *PLoS One* **11**(2): e0149403.
- 642 Sutter, N. B., D. S. Mosher, M. M. Gray and E. A. Ostrander (2008). "Morphometrics within dog breeds are highly
643 reproducible and dispute Rensch's rule." *Mamm Genome* **19**(10-12): 713-723.
- 644 Thompkins, A. M., B. Ramaiahgari, S. Zhao, S. S. R. Gotoor, P. Waggoner, T. S. Denney, G. Deshpande and J. S.
645 Katz (2018). "Separate brain areas for processing human and dog faces as revealed by awake fMRI in dogs (*Canis*
646 *familiaris*)." *Learn Behav* **46**(4): 561-573.
- 647 Tonoike, A., M. Nagasawa, K. Mogi, J. A. Serpell, H. Ohtsuki and T. Kikusui (2015). "Comparison of owner-
648 reported behavioral characteristics among genetically clustered breeds of dog (*Canis familiaris*)." *Sci Rep* **5**: 17710.
- 649 Tovote, P., J. P. Fadok and A. Luthi (2015). "Neuronal circuits for fear and anxiety." *Nat Rev Neurosci* **16**(6): 317-
650 331.
- 651 Vage, J., T. B. Bonsdorff, E. Arnet, A. Tverdal and F. Lingaas (2010). "Differential gene expression in brain tissues
652 of aggressive and non-aggressive dogs." *BMC Vet Res* **6**: 34.
- 653 Winkler, A. M., G. R. Ridgway, M. A. Webster, S. M. Smith and T. E. Nichols (2014). "Permutation inference for
654 the general linear model." *Neuroimage* **92**: 381-397.

655 Xu, L., K. M. Groth, G. Pearlson, D. J. Schretlen and V. D. Calhoun (2009). "Source-based morphometry: the use of
656 independent component analysis to identify gray matter differences with application to schizophrenia." Hum Brain
657 Mapp **30**(3): 711-724.
658 Zhang, Y., M. Brady and S. Smith (2001). "Segmentation of brain MR images through a hidden Markov random
659 field model and the expectation-maximization algorithm." IEEE Trans Med Imag **20**(1): 45-57.
660

661

662 **Extended data: Figures 1-1 & 1-2**
663

664 **Figure 1-1.** Conceptual schematic of neuroimaging analysis.



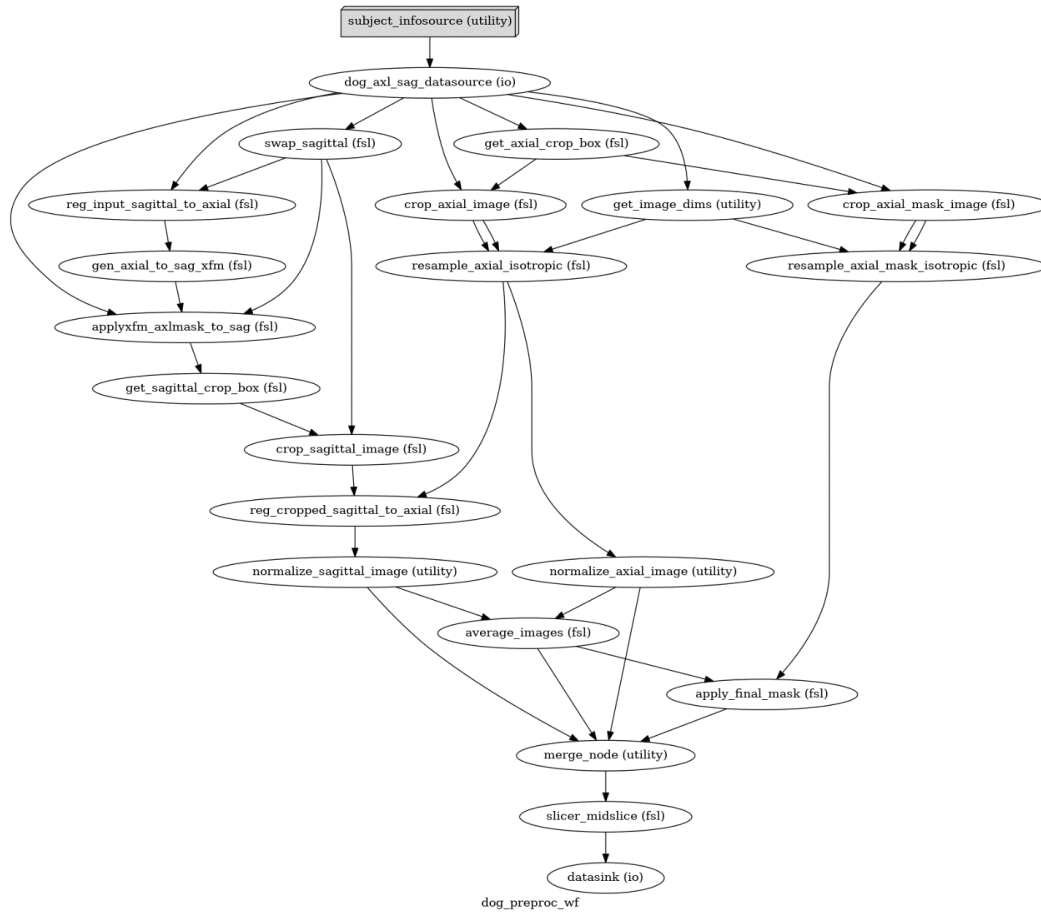
665

666

667 **Figure 1-2.** NiPype pipeline for merging axial and sagittal images from each dog before registration to
 668 the template. Code is available online at

669 <https://gist.github.com/dgutman/a0e05028fab9c6509a997f703a1c7413>.

670



671